Acta virologica **60**: 94 – 99, 2016 doi:10.4149/av_2016_01_94

Mapping of the regions involved in self-interaction of rice stripe virus P3 protein

S. L. ZHAO, J. H. HAO, Y. N. XUE, C. Y. LIANG

College of Bioscience and Biotechnology, Yangzhou University, 225009 Yangzhou, P. R. China

Received March 13, 2015; revised July 7, 2015; accepted January 25, 2016

Summary. – Rice stripe virus (RSV) protein P3 is a suppressor of RNA silencing in plants. P3 has been shown by biomolecular fluorescence complementation assay to self-interact *in planta* but the regions responsible for homotypic interaction have not been determined. Here we analyzed the domains for the self-interaction of P3 by using yeast two-hybrid, co-immunoprecipitation and fluorescence experiments. The results showed that P3 was also able to interact with itself in yeast and insect cells. The domain responsible for P3-P3 interaction was mapped to amino acids 15–30 at the N-terminal region of P3. Furthermore, subcellular localization suggested that the homo-oligomerization was the prerequisite for P3 to form larger protein aggregates in the nucleus of insect cell.

Keywords: rice stripe virus; P3; self-interaction; yeast two-hybrid; co-immunoprecipitation

Rice stripe virus (RSV), the prototype species of the genus *Tenuivirus*, causes a destructive disease of rice in East Asia (Wei *et al*., 2009). RSV is transmitted mainly by the small brown planthopper (SBPH), *Laodelphax striatellus* Falle´n, in a persistent, circulative-propagative manner (Deng *et al*., 2013). The genome of RSV consists of four single-stranded RNA segments (RNA1~4) containing seven open reading frames (Falk and Tsai, 1998). The complementary sense strand of RNA1 contains one ORF that encodes a putative viral RNA-dependent RNA polymerase (Toriyama *et al*., 1994). RNAs 2, 3 and 4 are ambisense and each contains two ORFs. One ORF is located in the 5' end of the viral sense RNA, while the other is in the 5' end of the viral complementary sense RNA (Falk and Tsai, 1998). Protein P3 encoded by the sense strand of RNA3 is a viral RNA silencing suppressor in plants (Xiong *et al*., 2009). P3 aggregates and forms inclusion bodies in *Spodoptera frugiperda* cells (Sf9) and RSV-infected plant tissues (Takahashi *et al*., 2003). A bimolecular fluorescence complementation (BiFC) assay has demonstrated that P3 could interact with itself in plants (Lian *et al*., 2014). But the important regions required for interaction have not been determined. Therefore, here we aim to determine the regions involved in self-interaction of P3 using yeast two-hybrid (Y2H), co-immunoprecipitation (co-IP) and fluorescence experiments.

To investigate whether P3 can interact with itself in yeast and insect cells, we first examined P3-P3 interaction using Y2H system in yeast cells and co-IP assay in Sf9 cells. In Y2H assay, the coding region of RSV P3 was cloned into pGADT7 in frame with the GAL4 activation domain and pGBKT7 in frame with the GAL4 DNA binding domain to generate prey plasmid pAD-P3 and bait plasmid pBD-P3, respectively. *Saccharomyces cerevisiae* AH109 cells were co-transformed with pAD-P3 and pBD-P3 and then plated on SD/-leu/-trp and SD/-leu/-trp/-his/-ade/X-α-gal medium. Yeast cells co-transformed with the plasmids pADT7-T and pGBKT7-Lam, pAD-P3 and pGBKT7, pADT7 and pBD-P3 were used as the negative controls, whereas yeast cells co-transformed with the plasmids pADT7-T and pGBKT7-53 were used as a positive control. All of these transformed yeast cells could grow on SD/-leu/-trp, indicating that they contain the respective bait and prey plasmids (Fig. 1a). Moreover, the respective protein expression could be detected by western

E-mail: slzhao@yzu.edu.cn; phone: +86-514-87991556.

Abbreviations: co-IP = co-immunoprecipitation; RSV = rice stripe virus; Y2H = yeast two-hybrid system

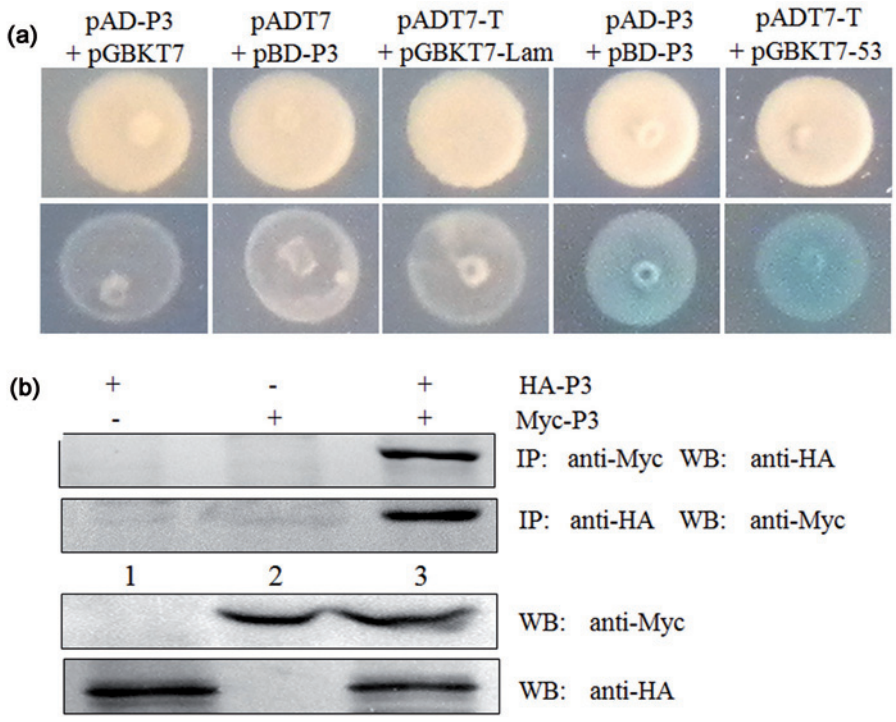

Fig. 1

Self-interaction of RSV P3 as demonstrated by Y2H and co-IP assays

(a) P3-P3 interaction in yeast two hybrid system. Yeast cells were co-transformed with each pair of prey and bait plasmids indicated above and plated on SD/-leu/-trp (upper panel) and SD/-leu/-trp/-his/-ade/X-α-gal medium (lower panel), respectively. (b) Co-immunoprecipitation analysis of P3-P3 interaction. Sf9 cells were infected with recombinant baculoviruses expressing HA-tagged P3 (lane1), Myc-tagged P3 (lane 2), or both (lane 3). At 72 hr post infection, the cell lysates were directly subjected to western blot (lower panels) or co-immunoprecipitation analysis (upper panels).

blot using anti-HA or anti-Myc monoclonal antibody (data not shown). Yeast cells co-transformed with pAD-P3 and pBD-P3 could grow on SD/-leu/-trp/-his/-ade/X-α-gal plate and turn blue as the positive control (pADT7-T and pGBKT7-53) (Fig. 1a). In contrast, no growth was observed on SD/-leu/-trp/-his/-ade/X-α-gal plate when the yeast cells were co-transformed with pAD-P3 and the empty bait vector pGBKT7, pBD-P3 and the empty prey vector pADT7, or the negative control (pADT7-T and pGBKT7-Lam) (Fig. 1a). These results indicated that P3 was able to interact with itself in yeast cells. In co-IP assay, Sf9 cells were co-infected with two recombinant baculoviruses expressing P3 fused with HA-tag (HA-P3) and P3 fused with Myc-tag (Myc-P3). At 72 hr post infection, the cells were lysed and subjected to immunoprecipitation with anti-HA or anti-Myc antibody (Beyotime). Lysates from cells infected with either one baculovirus were used as controls. Western blot revealed that HA-P3 and Myc-P3 were successfully expressed (Fig. 1b). Western blot of the precipitated proteins revealed that HA-P3 and Myc-P3 specifically co-immunoprecipitated (Fig. 1b), while no Myc-P3 was precipitated with anti-HA antibody and no HA-P3 was precipitated with anti-Myc antibody from control lysates (Fig. 1b). The co-IP results confirmed that P3 had the ability to self-interact in insect cells. Therefore, the data provided in this study and previous report (Lian *et al.*, 2014) demonstrated that P3 could interact with itself in yeast, insect and plant cells.

Coiled coils are well-known protein-interacting modules and have been found to mediate the interactions of many proteins (Moller *et al.*, 2005; DiCarlo *et al.*, 2007; Alminaite *et al.*, 2008). According to the coiled coils prediction program (Lupas *et al.*, 1991), one coiled-coil (15~30 aa) was predicted with a probability of 0.5 using the window size 14 residues (Fig. 2a). Secondary structure predictions using Distill 2.0 (Pollastri *et al.*, 2007) showed that the N-terminal 50 amino acids of P3 folds into two alpha-helices: the first helix includes residues 15 to 20, and the second one includes residues 37 to 48 (Fig. 2b). Based on the predictions, we generated six deleted mutants of P3 (Fig. 3a) and examined their interactions with wild-type P3 by using Y2H and co-IP. As shown in Fig. 3b, the N-terminally deleted mutant AD-P3-ΔN14 activated the expression of the reporter genes when co-expressed with the wild-type BD-P3, indicating that P3-ΔN14 was capable of interacting with P3. In contrast, no

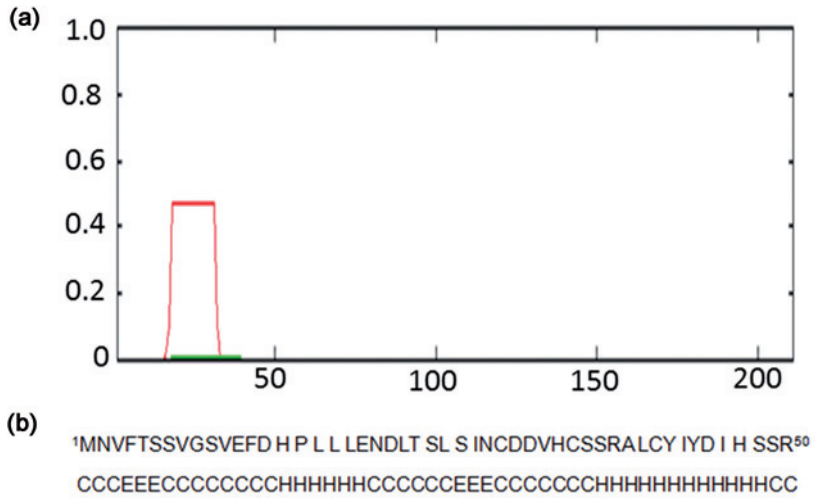

Fig. 2

Bioinformatic analysis of RSV P3 protein
(a) Coiled-coil prediction of P3. (b) The secondary structure prediction of P3.

growth on SD/-leu/-trp/-his/-ade/X-α-gal plate demonstrated that neither the N-terminally deleted mutant P3-ΔN30 nor P3-ΔN50 was able to interact with P3 (Fig. 3b). All the C-terminally deleted mutants, AD-P3-ΔC10, AD-P3-ΔC30 and AD-P3-ΔC80 could activate the reporter gene expression when co-expressed with BD-P3, demonstrating that the C-terminal 80 amino acids were not essential for P3-P3 interaction (Fig. 3b). These results indicated that the N-terminal region of 15–30 aa was essential for the P3-P3 interaction. To confirm the results obtained with Y2H analysis, we then examined the interaction between P3 and its deleted mutants by co-IP. Recombinant baculoviruses encoding each of the P3 mutants fused with Myc-tag were co-infected with the HA-P3-expressing baculovirus. Western blot analysis of the cell lysates using either anti-HA or anti-Myc antibody confirmed that all the mutants were expressed correctly (Fig. 3c). Additional aliquots of the cell extracts were incubated with anti-HA or anti-Myc antibody, and the precipitated proteins were analyzed by immunoblotting using anti-Myc or anti-HA antibody. As shown in Fig. 3c, the mutants P3-ΔN14, P3-ΔC10, P3-ΔC30 and P3-ΔC80 co-immunoprecipitated with HA-P3, while the mutants P3-ΔN30 and P3-ΔN50 could not co-immunoprecipitate with HA-P3, indicating that the region 15–30 aa of P3 was required for P3-P3 interaction. Thus the results obtained with the co-IP were in agreement with those of the Y2H assay: the N- terminal 15–30 aa was essential for the P3-P3 interactions.

To study the intracellular localization and whether there are differences in the staining pattern in insect cells, we fused the enhanced green fluorescence protein (eGFP) to the C-terminus of each intact and truncated P3 protein, expressed in Sf9 cells using baculovirus expression system, and examined by the confocal microscopy. The nuclei were counterstained with 4', 6-diamidino-2-phenylindole (DAPI). Intact P3 protein was localized predominately in the nucleus and formed larger aggregates (Fig. 4). Of the N-terminal truncations, P3-ΔN14 did not have a major effect on the appearance of the stained protein aggregates. However, the staining pattern of P3-ΔN30 or P3-ΔN50 differed from that of intact P3 remarkably: nearly no large protein aggregates were observed in Sf9 cells expressing P3-ΔN30 or P3-ΔN50 (Fig. 4). Of the C-terminal truncations, the staining pattern of P3-ΔC10 resembled that of intact P3. P3-ΔC30 and P3-ΔC80 were also able to form larger aggregates, although their aggregations were slightly affected: the size of aggregates was smaller than that formed by intact P3. These results indicated that P3 was targeted to the nucleus and deletion of N-terminal 15–30 aa of P3 impaired the formation of protein aggregates in cells.

In a previous report, RSV P3 was shown to accumulate predominantly in nuclei of plant cells through transient expression assay (Xiong *et al.*, 2009). Further analysis using immunocytochemistry and electron microscopy found that P3 proteins were localized in both nucleus and electron-dense amorphous inclusion bodies (AIB) in the cytoplasm of RSV-infected rice cells. In another report, P3 were detected as punctate inclusions and co-localized with ribonucleoprotein particles in AIB in RSV-infected SBPH (a cell line from the small brown planthopper) cells (Ma *et al.*, 2013). Here, our localization studies showed that RSV P3 formed larger aggregate in the nucleus when expressed independently in Sf9 cells. So, it was apparent that P3 was mainly localized in

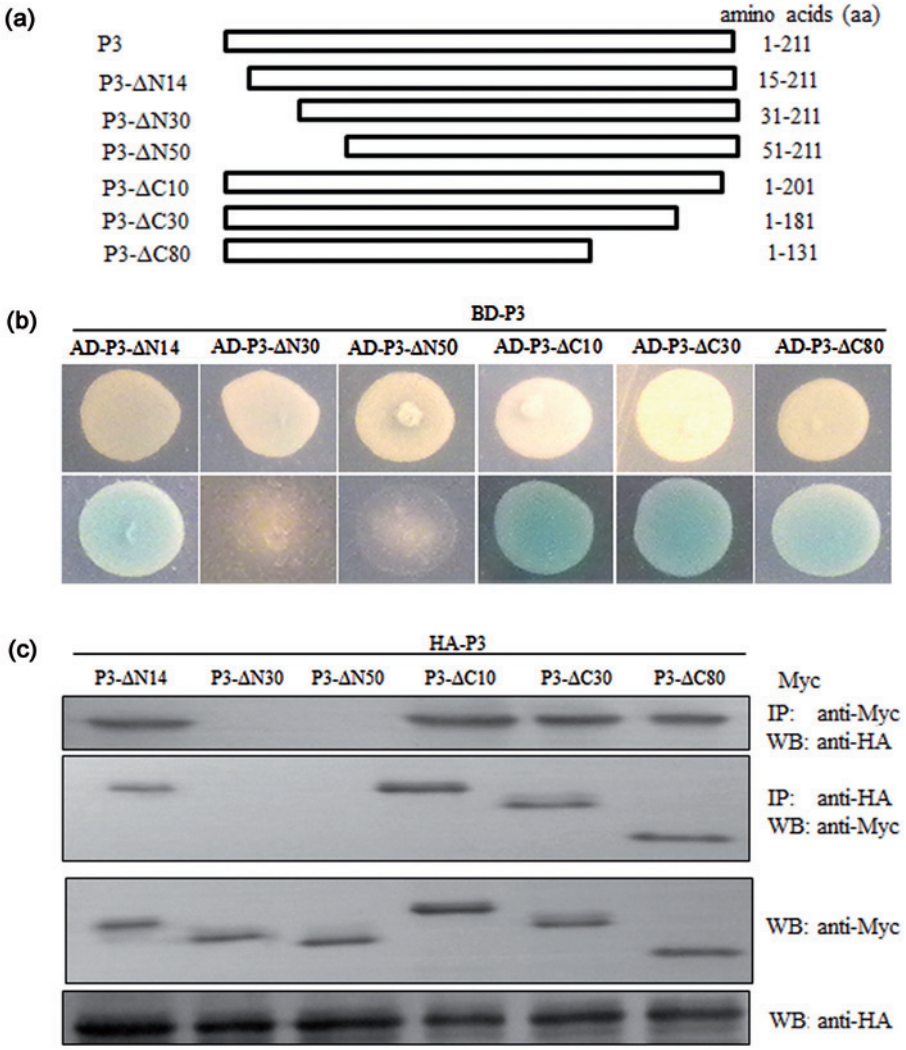

Fig. 3

Mapping the regions involved in RSV P3 self-interaction

(a) Schematic representation of P3 and its mutants. The amino acids (aa) of P3 included in each protein are shown on the right. (b) Homologous interaction between intact P3 and P3 deletions in yeast two hybrid system. Yeast cells were co-transformed with the bait plasmid pBD-P3 along with each of the prey plasmids as shown above and plated on SD/-leu/-trp (upper panel) and SD/-leu/-trp/-his/-ade/X-α-gal (lower panel) medium, respectively. (c) Co-immunoprecipitation of each P3 truncations with intact P3. HA-tagged P3 was co-expressed with Myc-tagged P3 deletion mutants in Sf9 cells. Cell extracts were subjected to western blot analysis with anti-Myc or anti-HA antibody directly (lower lanes) or after (upper lanes) being immunoprecipitated with anti-HA or anti-Myc antibody.

the nucleus when it was expressed solely in plant or insect cells, whereas it mainly localized in AIB in the cytoplasm of RSV-infected cells when other RSV-encoded proteins were present. Therefore, we speculate that the subcellular localization of P3 is possibly affected by other proteins encoded by RSV.

Homo-oligomerization was often found in viral structural proteins, which played important roles in viral replication, encapsidation and virus particle assembly (Moller *et al.*, 2005; Zhang *et al.*, 2008; Paul *et al.*, 2011). In addition to viral structural proteins, homo-oligomerization was also found in viral nonstructural proteins that aggregate to become functional *in vivo* such as some viral silencing suppressors. The crystallographic data suggest that Tombusviral P19 protein forms a head-to-tail homodimer to sequester siRNA duplex and prevents siRNA duplex loading into RISC (Ye *et al.*, 2003), flock house virus B2 protein forms a four-helix bundle homodimer to prevent siRNA duplex formation as well as siRNA duplex loading into RISC (Lingel *et al.*, 2005), and tomato aspermy virus 2b forms a pair of hook-like dimers

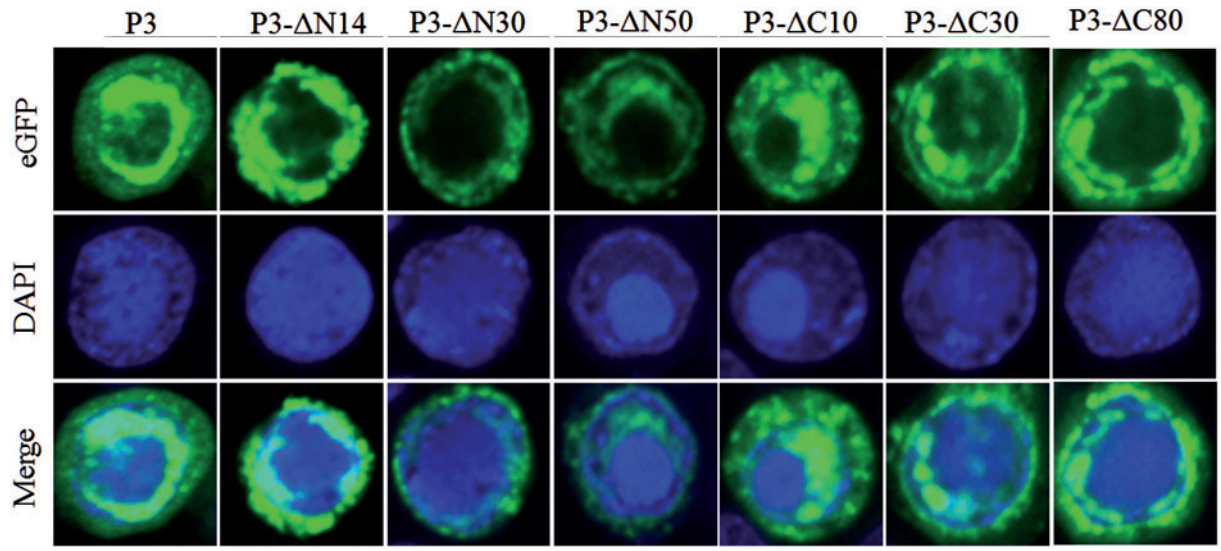

Fig. 4

Distribution of P3 and P3 truncations in Sf9 cells

Intact P3 and P3 deletion mutants were fused with eGFP at the C-teminus and expressed in Sf9 cells. The fluorescence was examined using confocal microscopy. The nuclei were counterstained with 4', 6-diamidino-2-phenylindole (DAPI).

to recognize the siRNA duplex in a sequence-independent manner (Chen *et al.*, 2008). Recently, studies on cucumber mosaic virus 2b protein demonstrated that self-interaction of 2b protein was crucial to its ability to suppress silencing and induce a symptom-like phenotype (Xu *et al.*, 2013). RSV P3 was identified as a viral silencing suppressor and it could suppress RNA silencing possibly through sequestering siRNA molecules. It is unknown whether RSV P3 also requires self-interaction to become a functional suppressor of silencing. The relevance of suppressor activity to self-interaction needs further study.

In summary, RSV P3 is able to self-interact *in vivo* and form large aggregates in the nucleus of insect cells. The predicted N-terminal coiled coil domain is responsible for the homotypic interaction of P3. The deletion mutants without this domain lose the ability to interact with wild type P3 as revealed by Y2H and co-IP experiments. Subcellular localization showed that deletion of self-interaction region did not affect the nuclear localization of P3 but compromised its capability of aggregation.

Acknowledgements. This research was supported by Natural Science Foundation of Jiangsu Province (BK20130441).

References

Alminaite A, Backstorm V, Vaheri A, Plyusmin A (2008): Oligomerization of hantaviral nucleocapsid protein: charged residues in the N-terminal coiled-coil domain contribute to intermolecular interactions. J. Gen. Virol. 89, 2167–2174. http://dx.doi.org/10.1099/vir.0.2008/004044-0

Chen HY, Yang J, Lin CQ, Yuan YA (2008): Structural basis for RNA-silencing suppression by tomato aspermy virus protein 2b. EMBO Rep. 9, 754–760. http://dx.doi.org/10.1038/embor.2008.118

Deng JH, Li S, Hong J, Ji YH, Zhou YJ (2013): Investigation on subcellular localization of rice stripe virus in its vector small brown planthopper by electron microscopy. Virol. J. 10, 310. http://dx.doi.org/10.1186/1743-422X-10-310

DiCarlo A, Moller P, Lander A, Kolesnikova L, Becker S (2007): Nucleocapsid formation and RNA synthesis of Marburg virus is dependent on two coiled coil motifs in the nucleoprotein. Virol. J. 4, 105–112. http://dx.doi.org/10.1186/1743-422X-4-105

Falk BW, Tsai JH (1998): Biology and molecular biology of viruses in the genus tenuivirus. Annu. Rev. Phytopathol. 36, 139–163. http://dx.doi.org/10.1146/annurev.phyto.36.1.139

Lian S, Cho WK, Jo YH, Kim SM, Kim KH (2014): Interaction study of rice stripe virus proteins reveals a region of the nucleocapsid protein (NP) required for NP self-interaction and nuclear localization. Virus Res. 183, 6–14. http://dx.doi.org/10.1016/j.virusres.2014.01.011

Lingel A, Simon B, Izaurralde E, Sattler M (2005): The structure of the flock house virus B2 protein, a viral suppressor of RNA interference, shows a novel mode of double-stranded RNA recognition. EMBO Rep. 6, 1149–1155. http://dx.doi.org/10.1038/sj.embor.7400583

Lupas A, van Dyke M, Stock J (1991): Predicting coiled coils from protein sequences. Science 252, 1162–1164. http://dx.doi.org/10.1126/science.252.5009.1162

Ma YY, Wu W, Chen HY, Liu QF, Jia DS, Mao QZ, Wu ZJ, Wei TY (2013): An insect cell line derived from the small brown planthopper supports replication of rice stripe virus, a tenuivirus. J. Gen. Virol. 94, 1421–1425. http://dx.doi.org/10.1099/vir.0.050104-0

Moller P, Pariente N, Klenk HD, Becker S (2005): Homo-oligomerization of Marburgvirus VP35 is essential for its function in replication and transcription. J. Virol. 79, 14876–14886. http://dx.doi.org/10.1128/JVI.79.23.14876-14886.2005

Paul D, Romero-Brey I, Gouttenoire J, Stoisova S, Krijnse-Locker J, Moradpour D, Bartenschlager R (2011): NS4B self-interaction through conserved C-terminal elements is required for the establishment of functional Hepatitis C virus replication complexes. J. Virol. 85, 6963–6976. http://dx.doi.org/10.1128/JVI.00502-11

Pollastri G, Martin AJ, Mooney C, Vullo A (2007): Accurate prediction of protein secondary structure and solvent accessibility by consensus combiners of sequence and structure information. BMC Bioinformatics 8, 201–212. http://dx.doi.org/10.1186/1471-2105-8-201

Takahashi M, Goto C, Ishikawa K, Matsuda I, Toriyama S, Tsuchiya K (2003): Rice stripe virus 23.9 K protein aggregates and forms inclusion bodies in cultured insect cells and virus-infected plant cells. Arch. Virol. 148, 2167–2179. http://dx.doi.org/10.1007/s00705-003-0171-0

Toriyama S, Takahashi M, Sano Y, Shimizu T, Ishihama A (1994): Nucleotide sequence of RNA1, the largest genomic segment of rice stripe virus, the prototype of the tenuiviruses. J. Gen. Virol. 75, 3569–3579. http://dx.doi.org/10.1099/0022-1317-75-12-3569

Wei TY, Yang JG, Liao FR, Gao FL, Lu LM, Zhang XT, Li F, Wu ZJ, Lin QY, Xie LH, Lin HX (2009): Genetic diversity and population structure of rice stripe virus in China. J. Gen. Virol. 90, 1025–1034. http://dx.doi.org/10.1099/vir.0.006858-0

Xiong RY, Wu JX, Zhou YJ, Zhou XP (2009): Localization of an RNA silencing suppressor encoded by Rice stripe tenuivirus. Virology 387, 29–40. http://dx.doi.org/10.1016/j.virol.2009.01.045

Xu A, Zhao Z, Chen W, Zhang H, Liao Q, Chen J, Carr JP, Du Z (2013): Self-interaction of the cucumber mosaic virus 2b protein plays a vital role in the suppression of RNA silencing and the induction of viral symptoms. Mol. Plant Pathol. 14, 803–812. http://dx.doi.org/10.1111/mpp.12051

Ye K, Malinina L, Patel D J (2003): Recognition of small interfering RNA by a viral suppressor of gene silencing. Nature 426, 874–878. http://dx.doi.org/10.1038/nature02213

Zhang X, Gree TJ, Tsao J, Qiu SH, Luo M (2008): Role of intermolecular interactions of vesicular stomatitis virus nucleoprotein in RNA encapsidation. J. Virol. 82, 674–682. http://dx.doi.org/10.1128/JVI.00935-07